JOURNAL OF MATERIALS SCIENCE 22 (1987) 532–538

Deformation behaviour of coextruded multilayer composites with polycarbonate and poly(styrene-acrylonitrile)

B. L. GREGORY, A. SIEGMANN,* J. IM,‡ A. HILTNER, E. BAER
Department of Macromolecular Science, Case Western Reserve University, Case Institute of Technology, Cleveland, Ohio 44106, USA

The tensile properties of coextruded multilayer composites comprised of predominantly 49 alternating layers of polycarbonate (PC) and polystyrene-acrylonitrile (SAN) were investigated in the bulk and microscopically. The bulk was characterized by three types of behaviour: brittle fracture at low strains, ductile yielding with fracture during neck formation, and formation of a stable neck followed by drawing to high extension. Optical microscopy was utilized to correlate deformation mechanisms within each phase to the observed modes of deformation in the bulk. Optical microscopy showed that in all cases the initial irreversible deformation event was the formation of cracks or crazes in the SAN layers. Good adhesion between the layers resulted in the subsequent initiation of shear bands in the polycarbonate layers at the craze tips. Interaction of crazes and shear bands produced an expanded damage zone ahead of the propagating crack which delocalized the stress and delayed fracture. The ultimate mode of fracture depended on the relative thickness of the SAN and PC layers, as determined by the composition, and the strain rate.

1. Introduction

Coextrusion is one way in which two or more polymers can be physically combined for the purpose of achieving improved properties. Alfrey and Schrenk and co-workers have described the technologies involved in the production of multilayer composites as well as the physical properties of these systems [1–9]. This paper is specifically concerned with the mechanical behaviour which results when a brittle polymer such as styrene-acrylonitrile (SAN) is combined with a tough ductile polymer such as polycarbonate (PC) in a multilayer composite. This system differs from most physical blends in that within the plane of the sheet, both phases are continuous. It has been shown in another publication that this condition of cocontinuous phases gives rise to a new relaxation peak at a temperature intermediate to the two glass transition peaks [10].

The two polymers of interest here are nearly immiscible although Paul and Newman have shown that sufficient intermixing occurs to produce good adhesion [11]. As a result, stresses are readily transferred from one layer to another and synergistic effects may be produced. In this study, the bulk mechanical properties of 49 and 193 layer sheets of alternating PC and SAN were examined. Subsequently, microdeformation studies were undertaken in the optical microscope in order to probe the nature of irreversible microdeformation processes and the role of interfacial adhesion.

2. Experimental technique

Multilayer composite sheets comprised of alternating layers of polycarbonate (PC) and a styrene-acrylonitrile copolymer (SAN) with 25% acrylonitrile by weight were prepared by the Dow Chemical Company using the multilayer coextrusion process previously described by Alfrey and Schrenk and co-workers [1–9]. The SAN composition was chosen for maximum adhesion to PC [11]. Polycarbonate serves as the outer layer in all of the composites, the 49 layer system is comprised of 25 layers of PC and 24 layers of SAN, the 193 layer system of 97 layers of PC and 96 layers of SAN. The overall thickness of the sheets is approximately 1/16 in ($\sim$ 1.58 mm) so that compositional changes are reflected by changes in the relative layer thickness of each phase. Samples of PC alone and SAN alone were prepared by the same coextrusion process as the composites and served as the controls for the experiments. Although prepared from the same coextrusion process, the controls did not display the layered structure of the composites.

Tensile specimens were milled from the multilayer sheets. The standard ASTM D638 geometry was modified by tapering the centre of the gauge length by 0.002 in ($\sim$ 0.05 mm) to localize failure in the centre of the specimen. Tensile tests were performed on a standard Instron Testing Machine at three strain rates: 0.58, 2.9 and 58% min^{-1}. Modulus measurements were obtained with an extensometer at strains no

*On sabbatical leave, Technion-Israel Institute of Technology, Department of Materials Engineering, Haifa, Israel.
‡*Present address*: Dow Chemical Company, Midland, Michigan 48650, USA.

0022–2461/87 $03.00 + .12

TABLE I Tensile properties of 49 layer PC/SAN composites

Strain rate (% min^{-1})	Composition (wt % PC)	Modulus (GPa)	Yield stress (MPa)	Yield strain (%)	Fracture stress (MPa)	Fracture strain (%)
0.58	100	2.43	60.2	6.8	–	81.3
	65	2.64	62.3	5.8	–	23.9
	54	2.78	64.0	5.4	–	19.9
	40	2.92	65.0	5.3	–	9.6
	27	3.20	–	–	68.8	4.8
	0	3.34	–	–	67.3	3.7
2.9	100	2.36	64.0	6.8	–	85.0
	65	2.50	57.6	5.6	–	15.1
	54	2.71	65.3	5.8	–	6.7
	40	2.78	–	–	68.5	5.4
	27	3.06	–	–	73.7	4.7
	0	3.34	–	–	71.4	3.8
58	100	2.32	63.1	6.7	–	92.8
	65	2.77	65.0	5.6	–	37.2
	54	2.80	65.3	5.5	–	7.3
	40	3.01	–	–	68.9	5.2
	27	3.23	–	–	70.2	4.5
	0	3.43	–	–	72.1	4.0

greater than 0.5%. The test was repeated five times on each specimen and the average value reported.

Specimens for the optical microscope were milled from the edge of the multilayer sheets. The 20 mil (50.8×10^{-2} mm) specimens were polished initially with emery paper then on a metallurgical wheel with successively finer grades of alumina powder in water. The final polishing was made with 0.05 μm alumina. Notches were introduced by drawing a razor blade across the edge through the first few layers. Notched and unnotched specimens were clamped in a stretching device which was calibrated to 0.0002 in ($\sim$ 0.005 mm) in displacement. The device was mounted in the optical microscope and photographs were taken as the specimen was deformed. Polarizing plates crossed at 45° were used to observe strain birefringence and for greater contrast in viewing shear processes in the PC layers.

3. Results and discussion

The moduli of both the 49 layer composites and the two controls at three strain rates are shown in Table I. The average values for the SAN the the PC controls, 3.34×10^9 and 2.43×10^9 Pa, respectively, correspond well with the values given in the literature. Experimental values for the four compositions intermediate to the two controls indicate that the modulus follows the law of mixtures.

Table I also shows the tensile properites of the 49 layer PC/SAN system. The data represent the average values of at least five runs. Short crazes initially developed in the SAN control along the edges of the specimens at approximately 1% strain. The craze density increased with increasing elongation as crazes appeared in the centre of the specimens. The SAN control failed in a brittle manner at a strain of 3 to 4%. The PC control exhibited ductile behaviour. During initial stages of deformation macro shear bands formed along the edges of the specimen. The shear bands increased in size until at the yield point several shear bands coalesced and formed a sharp neck that extended diagonally across the specimen. The neck formed at strains of 7 to 9%. Failure occurred at extensions well over 100% after considerable cold drawing.

The composites showed intermediate behaviour which depended on the composition. For 49 layers, the 27/73 (PC/SAN) composite failed at an average stress slightly higher than SAN and at strains of 4 to 5%. Optical micrographs showed that crazes occurred only in the SAN phase and extended across the entire width of the specimen. The crazes did not register from layer to layer, but were randomly dispersed through all the SAN layers. The 40/60 composition underwent local necking, but failed during the necking process, or shortly afterward, at strains of 7 to 9%. In both the 54/46 and 65/35 compositions a sharp neck formed and the specimens cold drew in a fashion analogous to the PC control, but failed at lower elongations.

The values shown in Table I depict the average behaviour of the composites, but the composites actually exhibited a broad range of behaviour within a single composition. Failure either occurred at low strains in a relatively brittle fashion or after considerable cold drawing in a ductile fashion. These two modes of failure are defined as Type A and Type B behaviour and as such are shown in Fig. 1. Type A behaviour is depicted as relatively brittle where the specimen fails either before yielding (A1) or during the formation of a neck (A2). Type B behaviour is depicted as ductile behaviour and is characterized by formation of a stable neck which cold draws.

Both Type A and B failure mechanisms were observed for those compositions in the brittle–ductile transition region. This bimodal failure of the intermediate compositions with 40 to 65% PC is shown in Figs 2 to 4 for the 49 layer composites at three strain rates. The filled and half-filled circles represent Types A1 and A2 behaviour, respectively, while the open circles correspond to Type B behaviour. At the highest strain rate only 65/35 specimens failed by both A and

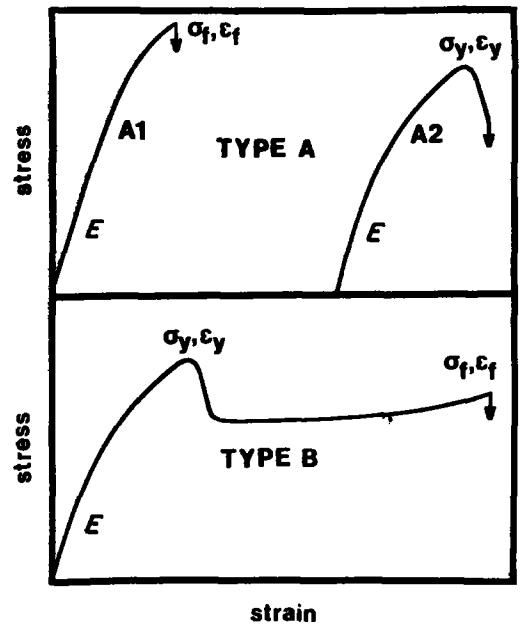

Figure 1 Schematic diagrams depicting the stress–strain relationship of Types A1, A2 and B behaviour.

B modes, but with decreasing strain rate failures showed more ductile behaviour. For example, at the intermediate strain rate both 54/46 and 65/35 showed bimodal failures and at the lowest strain rate both exhibited only ductile failures while the 40/60 showed indications of bimodal behaviour.

Compositions higher in polycarbonate were examined with 193 layer composites. These differ from the 49 layer composites only by the thickness of the layers since the overall thickness of the sheets is the same. Comparison of the 49 and 193 layer composites at a strain rate of 58% min^{-1} (Figs 4 and 5) suggests that the latter may be more ductile. This is most clearly seen with the intermediate compositions, for example the 40/60 composition is bimodal in 193 layers but only brittle in 49 layers, and the 67/33 composition is always ductile in 193 layers but the 65/35 composition is bimodal in 49 layers. This apparent effect of layer

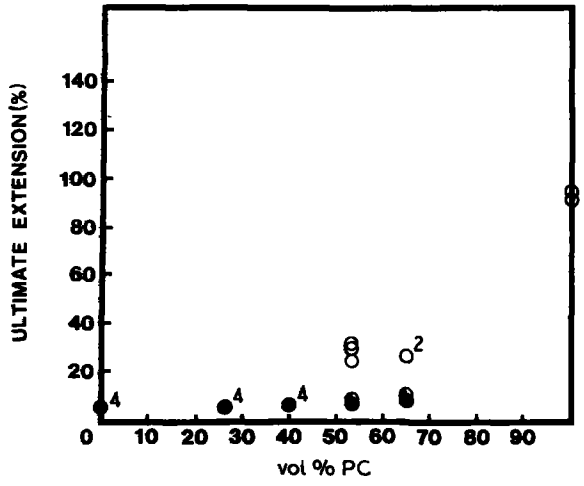

Figure 3 Ultimate extension (%) plotted against vol % PC for the 49 layer system at a strain rate of 2.9% min^{-1}. Symbols have the same meaning as in Fig. 2.

thickness will be examined further in a subsequent publication.

A larger number of compositions was examined in 193 layers in the composition range higher in polycarbonate where ductile failure occurs. The results clearly illustrate the increase in average fracture elongation with increasing PC content. The scatter in the data also increases because some specimens of all compositions including 90/10 fractured at very low strains, considerably lower than any of the PC controls. Since ductile failure occurs by neck formation, the fracture strain is a meaningful quantity only as it represents the stability of the neck in the cold drawing process. The wide distribution of fracture strains particularly the number of low values in Fig. 5 suggests that some of the composite sheets may contain macroscopic flaws or contaminants that were not completely purged prior to sample extrusion. The large scatter in fracture strain of the PC controls (Fig. 5) seems to support this view.

Optical microscopy was used to further examine the microdeformation processes which precede and control the transition from Type A to Type B behaviour.

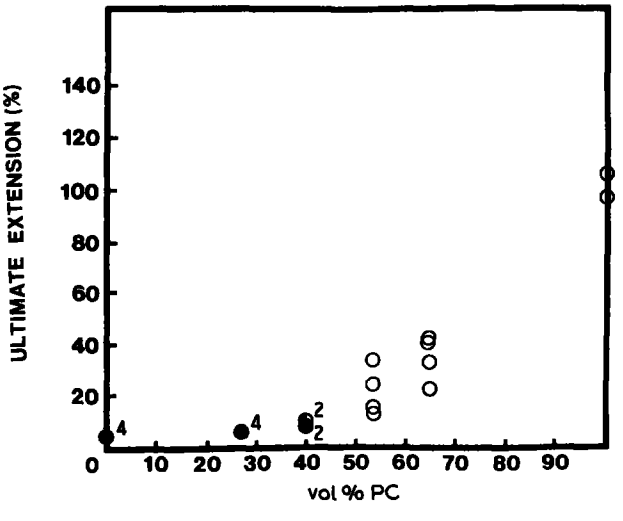

Figure 2 Ultimate extension (%) plotted against vol % PC for the 49 layer system at a strain rate of 0.58 % min^{-1}. (●) Type A1 fracture; (◐) Type A2 fracture; (○) Type B fracture. The small numbers indicate the number of specimens tested.

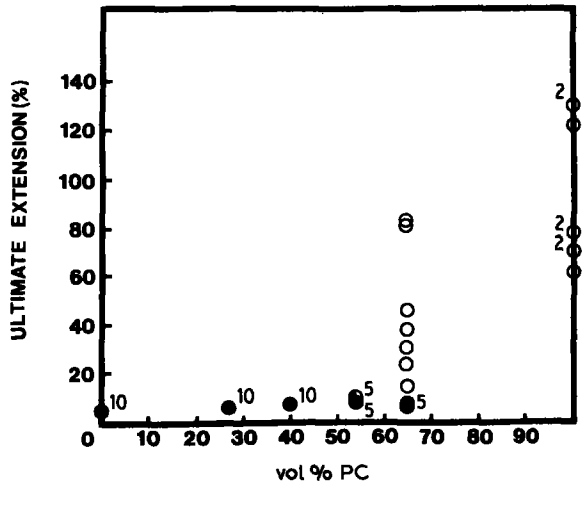

Figure 4 Ultimate extension (%) plotted against vol % PC for the 49 layer system at a strain rate of 58% min^{-1}. Symbols have the same meaning as in Fig. 2.

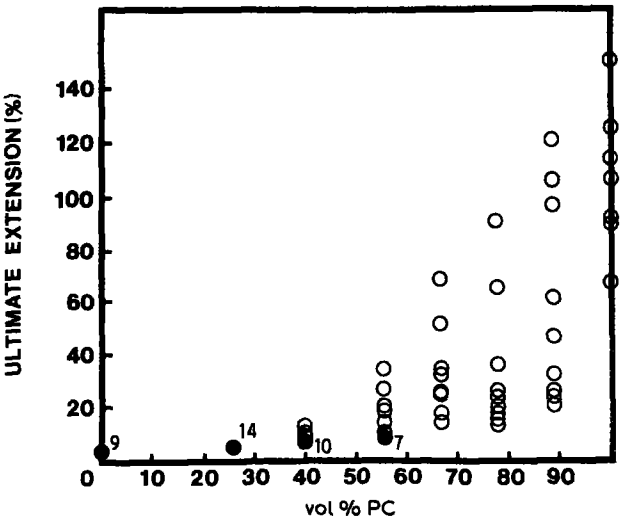

Figure 5 Ultimate extension (%) plotted against vol % PC for the 193 layer system at a strain rate of 58% min^{-1}. Symbols have the same meaning as in Fig. 2.

By recording the evolution and interaction of crazing and shear processes as 49 layer microspecimens were strained under the optical microscope, it was possible to generate qualitative correlations between the development of microstructure and the behaviour of specimens in the bulk.

In the Type A regime, bulk behaviour is characterized by brittle fracture at relatively low extensions. While Type A behaviour was encountered occasionally in all compositions aside from the PC control, Type A behaviour predominates in ratios high in SAN. The first observable irreversible deformation event in the 27/73 composite is the development of isolated crazes at approximately 1% strain. These are referred to as crazes but could be cracks since the characteristic microfibrillar structure of crazes has not been confirmed. Crazing is observed exclusively in the SAN layers (Fig. 6a), no observable deformation has occurred in the PC layers. With further elongation more crazes develop in SAN layers. Damage appears to be isolated solely in the SAN layers up to this point. At higher strains, shear zones initiate from the craze tips into the PC layers. These shear zones extend through the PC layer and connect crazes in adjacent SAN layers (Fig. 6b). Subsequent failure is controlled by the thicker SAN layers since the fracture surfaces (Fig. 6c) show little evidence of drawing in the PC layers.

Initially Type B behaviour of the 65/35 composite proceeds much like Type A behaviour with the appearance of crazes in the SAN layers at approximately 1% strain (Fig. 7a). At higher strains the crazes initiate shear processes in the PC layers. Because the PC layers are thicker the shear zones do not initially extend across the entire width of the PC layers (Fig. 7b). Only after formation of additional shear zones at higher strains do the shear zones coalesce and extend across the PC layers as shown in Fig. 7c. In this composite, the shear bands are stable and the PC layers cold draw (Fig. 7d). The large extensions achieved in the PC layers are accommodated in the SAN layers by formation of large holes at the sites of crazes or cracks. From a qualitative comparison of Figs 7c and d it is apparent that the latter has undergone considerably larger strain. A lower magnification view of the fractured specimen (Fig. 8) shows that cold drawing of the microspecimens proceeds by neck formation as was also observed in the bulk specimens of this composition. The high extensions with accompanying hole formation are only observed in the necked region. A higher magnification view of the left side of the specimen in Fig. 8 would be similar to Fig. 7c while the right side would appear similar to Fig. 7d.

Good adhesion between layers maintains the integrity of the composite while the PC layers draw and holes form in the SAN layers. During the cold draw stage of deformation the interaction of the two phases is manifested by the diagonal alignment of holes in the SAN layers (Fig. 9). As the PC layers draw, the

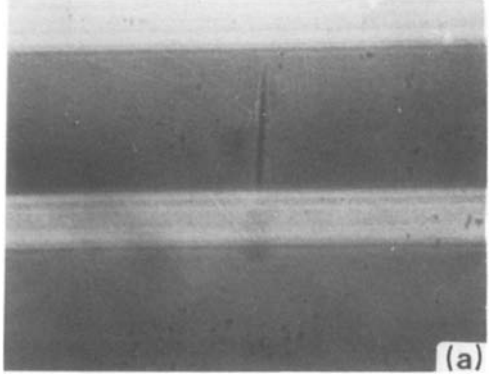

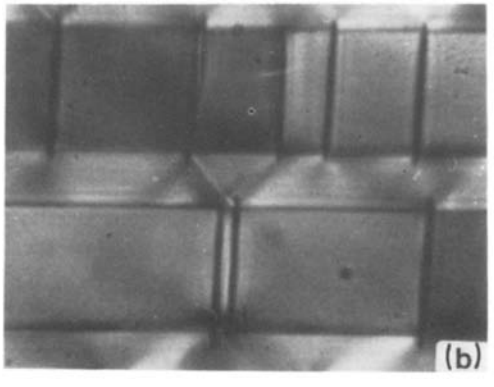

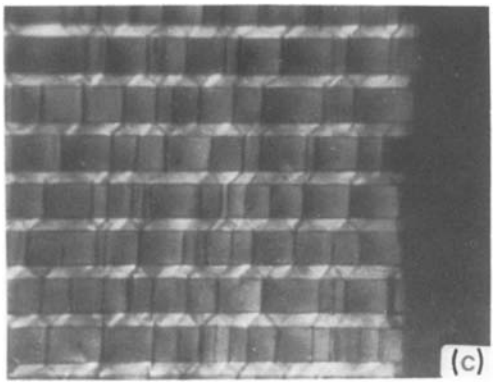

Figure 6 (a, b, c) Optical micrographs of a 27/73 PC/SAN specimen taken at different levels of strain. These micrographs correlate observed deformation morphologies with typical A1 behaviour. The PC and SAN layers are approximately 9 and 22 μm thick, respectively.

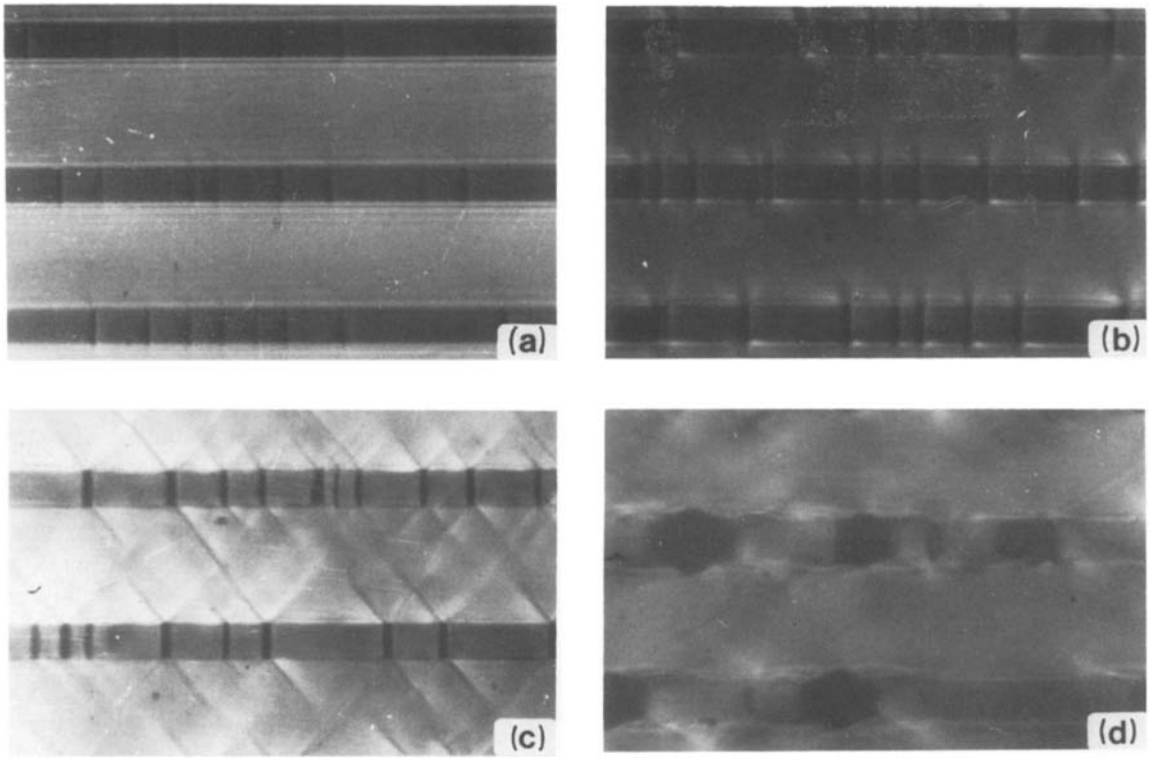

Figure 7 (a, b, c, d) Optical micrographs of a 65/35 PC/SAN specimen taken at four levels of strain to illustrate the deformation morphologies involved in Type B behaviour. The PC and SAN layers are approximately 44 and 13 μm thick, respectively.

adhering SAN blocks are pulled into staggered arrays angled at 45° to the direction of deformation. With greater strain PC layers begin to fail, holes in adjacent SAN layers coalesce to form larger voids and eventually the specimen fractures.

It has been seen that microdeformation mechanisms observed in the control polymers are maintained in the microlayer composities so that crazing occurs solely in the SAN layers and shear banding solely in the PC layers. Interaction between crazes and shear bands is the result of good adhesion between the layers. Subsequently crazes, or possibly cracks, that form in the SAN layers are blunted by the tough PC where they initiate shear bands. Ultimately the mode of failure is determined by the relative layer thickness of the two phases. Thicker SAN layers lead to brittle fracture and thicker PC layers lead to ductile behaviour. Depending on the strain rate and the composition ratio a transition from predominately Types A1 and A2 behaviour to Type B behaviour is encountered. In Type A2 and Type B behaviour the tough PC layers effectively diffuse stresses generated by the craze tips that originate in the SAN layers. This prevents brittle fracture and in the case of Type B behaviour allows the composite to form a stable neck which subsequently draws.

The following is a description of crack propagation in a notched microtensile specimen as it is deformed under the optical microscope. Fig. 10 illustrates crack growth and propagation in the 49 layer composite with 54/46 PC/SAN composition. The even-numbered layers are SAN while the odd-numbered layers are PC. The notch was introduced by drawing a razor blade across the top of the specimen. As was true of all

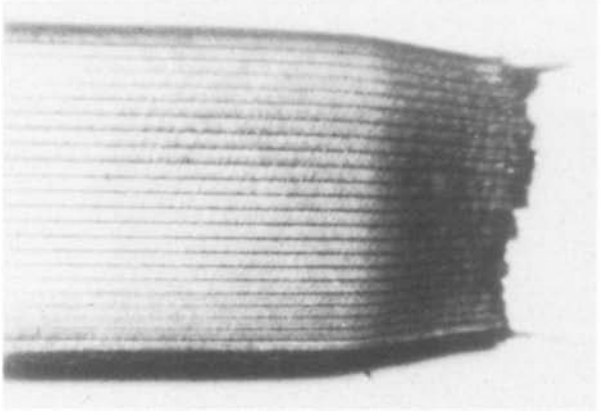

Figure 8 Optical micrograph of the fractured 65/35 PC/SAN specimen in Fig. 7.

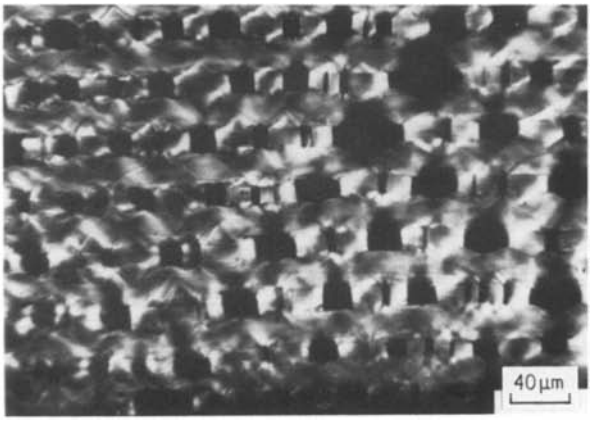

Figure 9 Optical micrograph of a drawn 65/35 PC/SAN specimen showing the diagonal alignment of holes in the SAN layers.

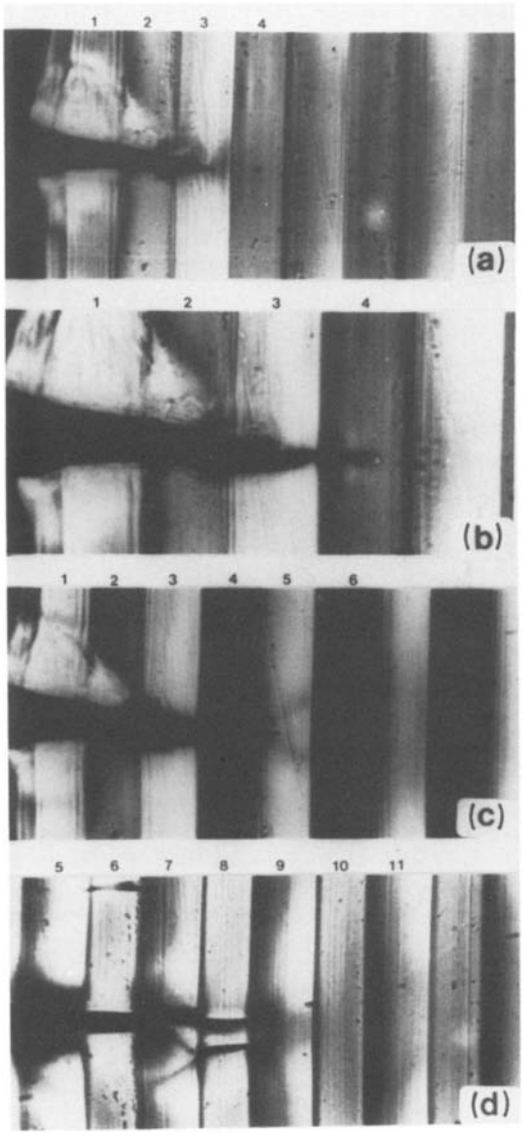

Figure 10 (a, b, c, d) Optical micrographs of a notched 54/46 PC/SAN specimen taken at different levels of strain. The PC and SAN layers are approximately 21 and 18 μm thick, respectively.

notched microspecimens the notch tip was halted in a PC layer. There was no evidence of delamination resulting from the notching process.

Fig. 10a was taken at a low strain prior to crack growth. The stress concentrations ahead of the notch tip are manifested as an oblong region of birefringent colours. Although best seen in colour photographs, the general shape of this zone is apparent in the black and white prints. Changes in stress during deformation were demonstrated by successive colour retardations within this zone. The continuous shape of the zone through many alternating layers of PC and SAN indicates that the adhesion is adequate for efficient transfer of the stresses.

In Fig. 10b a crack is developing in front of the notch tip. While there is doubt whether a crack has actually developed there is no question that plastic deformation has occurred in the black region ahead of the original notch. In other notched specimens taken to similar levels of strain, damage was found to be irreversible. The plastic deformation extends into the SAN layer (labelled 4) ahead of the notch. Immediately after the photograph in Fig. 10b was taken, the crack moved to the position in 10c. The crack has passed through the SAN layer (labelled 4) and is blunted in the next PC layer (labelled 5). Considerable plastic deformation accumulates in this PC layer before propagation again occurs with a sudden jump through the next SAN layer (labelled 6). The initial mode of crack propagation – damage accumulation in a PC layer followed by rapid propagation through an SAN layer and arrest in the next PC layer – is modified as crack growth proceeds. In Fig. 10d two cracks or crazes have developed in SAN layers away from the primary crack. The crack closest to the main propagating crack serves to diffuse the stress since the shape of the birefringent zone is broader and more complex. Shear zones in the PC layer have also initiated from the tip of the second crack in a manner which suggests that the PC layer (labelled 5) behind the crack tip has not fractured.

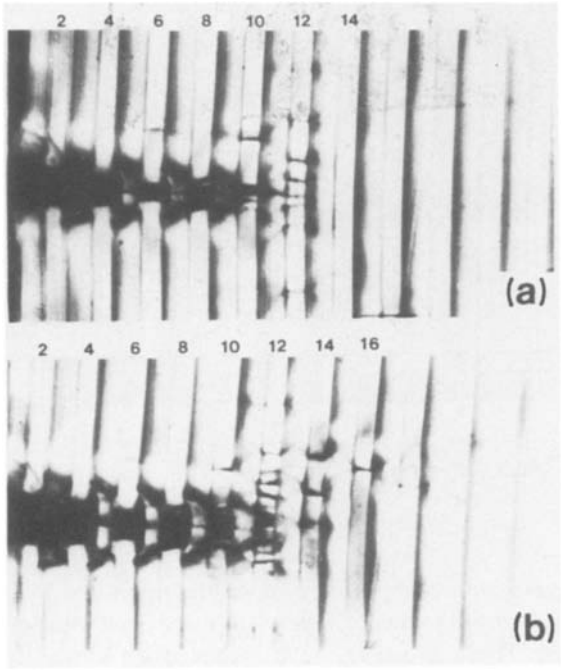

Figure 11 (a, b) Optical micrograph of the 54/46 PC/SAN specimen in Fig. 10 taken at higher levels of strain.

Damage becomes more delocalized as deformation proceeds with the formation of cracks away from the main crack and the subsequent development of shear zones in the PC layers. The end effect of these processes is the delocalization of stress that is manifested in the form of an expanded damage zone and delayed fracture. In Fig. 11a it can be seen that the PC layers do not fracture but rather undergo high levels of plastic deformation. These load-bearing PC layers which have drawn across the crack serve to delocalize stresses at the crack tip while also maintaining the physical integrity of the specimen. The drawing of the PC layers is fed from the bulk and results in observable delamination at the interfaces. At this point it is difficult to define the tip of the primary crack. The stresses have been delocalized to the point where there is no longer a primary advancing crack tip. In Fig. 11b the PC layers have drawn further and show greater levels of delamination. Cracking is profuse in the SAN

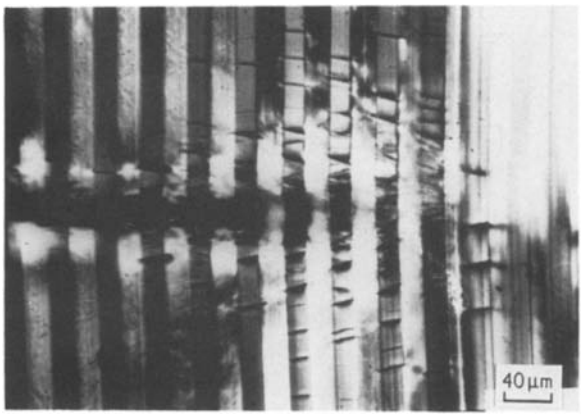

Figure 12 Optical micrograph of a 54/46 PC/SAN notched fatigue specimen prior to failure.

layers immediately in front of the main crack while shear zones in the PC layers originate from these crack tips. These processes have extended well away from the main crack tip area. The specimen is now on the verge of fracture. Fracture occurs as the individual PC layers break in an "unzipping" manner. The fractured specimens show that many of the PC layers delaminated and pulled out from the bulk specimen before they fractured.

Another notched specimen deformed in a cyclic fatigue mode is shown in Fig. 12. The damage zone is much larger than in specimens deformed in a single loading experiment. Cracks away from the main crack are tilted at an angle which aligns them with the lines of stress. Cracking ahead of the main crack is profuse to the point that individual cracks are barely discernable. Again, the SAN layers fracture as the crack propagates while the PC layers undergo large local deformation and remain intact.

4. Conclusions

This investigation of the mechanical properties of coextruded multilayer composites with 49 or 193 alternating PC and SAN layers leads to the following conclusions:

1. Three modes of failure can be identified: brittle fracture at low extensions (Type A1), fracture at low strains during neck formation (Type A2), and formation of a stable neck which cold draws and fractures at high strains (Type B). In the brittle–ductile transition region all three modes may be observed for a single composition.

2. At low strains, crazes in the SAN layers are blunted by the PC where they subsequently initiate shear bands. Type B behaviour occurs when the PC layers are able to undergo large extensions despite the formation of a network of holes in the SAN layers.

3. Interaction of the crazes and shear bands produces an extended damage zone ahead of the crack. This damage zone diffuses stresses and retards crack propagation.

Acknowledgement

The authors gratefully acknowledge the generous financial support of the Dow Chemical Company. The research was performed in the Center for Applied Polymer Research (CAPRI).

References

1. W. J. SCHRENK, US Patent 3 773 882 (1973).
2. W. J. SCHRENK and T. ALFREY Jr, *Soc. Plast. Eng. J.* **29** (1973) 38.
3. L. M. TOMKA and W. J. SCHRENK, *Mod. Plast.* **49** (1972) 62.
4. W. J. SCHRENK and T. ALFREY Jr, *Polym. Eng. Sci.* **9** (1969) 393.
5. T. ALFREY Jr, *Appl. Poly. Symp.* **24** (1974) 3.
6. T. ALFREY Jr, E. F. GURNEE and W. J. SCHRENK, *Polym. Eng. Sci.* **9** (1969) 400.
7. J. IM and W. F. SHRUM, US Patent 4 540 623 (1985).
8. J. A. RADFORD, T. ALFREY Jr and W. J. SCHRENK, *Polym. Eng. Sci.* **13** (1973) 216.
9. W. J. SCHRENK and T. ALFREY Jr, in "Polymer Blends", Vol. 2, edited by D. R. Paul and S. Newman, (Academic, New York, 1978) p. 129.
10. B. GREGORY, A. HILTNER, E. BAER and J. IM, *Polym. Eng. Sci.* (1986) in press.
11. J. D. KEITZ, J. W. BARLOW and D. R. PAUL, *Appl. Polym. Sci.* **29** (1984) 3131.

Received 17 March
and accepted 2 June 1986